Differential Expression Analysis of Cutaneous Squamous Cell Carcinoma and Basal Cell Carcinoma Proteomic Profiles Sampled with Electroporation-Based Biopsy

Edward Vitkin[1,2], Julia Wise[1], Ariel Berl[3], Ofir Shir-az[3], Batel Gabay[1], Amrita Singh[1], Vladimir Kravtsov[4], Zohar Yakhini[2,5], Avshalom Shalom[3] and Alexander Golberg[1]

Clinical misdiagnosis between cutaneous squamous cell carcinoma (cSCC) and basal cell carcinoma (BCC) affects treatment plans. We report a tissue sampling approach with molecular biopsy using electroporation. This method, coined electroporation-based biopsy (e-biopsy), enables nondestructive nonthermal permeabilization of cells in the skin for vacuum-assisted extraction of biomolecules. We used e-biopsy for ex vivo proteome extraction from 3 locations per patient in 21 cSCC, 20 BCC, and 7 actinic keratosis human skin samples. Using liquid chromatography with tandem mass spectrometry, we identified 5966 proteins observed with nonzero intensity in at least 1 sample. The intrapatient Pearson correlation of 0.888 ± 0.065 for patients with BCC, 0.858 ± 0.077 for patients with cSCC, and 0.876 ± 0.116 for those with solar actinic keratosis indicates high consistency of the e-biopsy sampling. The mass spectra presented significantly different proteome profiles for cSCC, BCC, and solar actinic keratosis, with several hundreds of proteins differentially expressed. Notably, our study showed that proteomes sampled with e-biopsy from cSCC and BCC lesions are different and that proteins of *CRNN*, *SULT1E1*, and *ITPK1* genes are significantly overexpressed in BCC in comparison with those in cSCC. Our results provide evidence that the e-biopsy approach could potentially be used as a tool to support cutaneous lesions classification with molecular pathology.

Keywords: Diagnostics, Finite elements modeling, Machine learning, Molecular pathology, Protein–protein interaction, Skin cancer

JID Innovations (2024);**4:**100304 doi:10.1016/j.xjidi.2024.100304

INTRODUCTION

Although the clinical features of cutaneous squamous cell carcinoma (cSCC) and basal cell carcinoma (BCC) are well-described, sometimes, the clinical phenotypes of these cancers are ambiguous, and discrepancies between the clinical presentations and histologic analyses occur (Neagu et al, 2020; Ryu et al, 2018). Misclassification of cSCC as BCC carries the highest risk to patients owing to the inherent potential for recurrence, metastases, and mortality (Lallas et al, 2015). Recent studies suggested that the introduction of molecular biomarkers, which accurately stratify non-melanoma skin lesions, would provide a new frontier in personalization of skin cancer care and hold a potential of greatly improving patient diagnosis in many cases (Azimi et al, 2020).

The current strategy for biomarkers sampling involves extraction of molecules using lyses buffers from tissue sampled with tissue biopsies. Such conventional tissue biopsy procedures carry risks involved with surgical procedures and may lead to localized tissue injury, bleeding, inflammation, infection, and scarring (Abhishek and Khunger, 2015). In addition, because of these risks, only a very few biopsies can be performed in a single procedure, limiting the scope of the spatial mapping of the entire lesion, potentially leading to misdiagnosis if the tumor is only partially sampled or completely missed (Wolberink et al, 2013).

Recently, we introduced a tissue sampling approach with molecular biopsy using electroporation. We have shown that such electroporation-based molecular sampling, termed electroporation-based biopsy (e-biopsy), selectively extracts liquids from solid tissues with informative proteomes in animal models in liver cancer (Golberg et al, 2019) and brain melanoma (Genish et al, 2022) in vitro and from breast cancer in vivo (Vitkin et al, 2022). In this study, we demonstrate the ability to sample the informative proteome by e-biopsy from excised human skin. Specifically, we show

[1]*Porter School of Environment and Earth Sciences, Tel Aviv University, Tel Aviv, Israel;* [2]*Efi Arazi School of Computer Science, Reichman University, Herzliya, Israel;* [3]*Department of Plastic Surgery, Meir Medical Center, Kfar Sava, Israel;* [4]*Department of Pathology, Meir Medical Center, Kfar Sava, Israel; and* [5]*Department of Computer Science, Technion - Israel Institute of Technology, Haifa, Israel*

Correspondence: Alexander Golberg, Center for Engineering in Medicine & Surgery, Department of Surgery, Massachusetts General Hospital, Harvard Medical School, 51 Blossom, Boston, Massachusetts 02114, USA. E-mail: agolberg@tauex.tau.ac.il

Abbreviations: AK, actinic keratosis; BCC, basal cell carcinoma; cSCC, cutaneous squamous cell carcinoma; e-biopsy, electroporation-based biopsy; iBAQ, intensity-based absolute quantification

Received 6 December 2023; revised 11 July 2024; accepted 12 July 2024; accepted manuscript published online XXX; corrected published online XXX

Cite this article as: JID Innovations 2024;4:100304

that proteomic profiles obtained by e-biopsy, between cSCC, BCC (malignant lesions), and solar actinic keratosis (AK) (benign lesion), are differentially expressed. Our e-biopsy approach to the characterization of skin tumors differs substantially from conventional excision biopsy approaches, which require tissue resection and which provide information limited to the size and the region of resected tissue. e-biopsy is also substantially different from direct mass spectrometric tools (Balog et al, 2013; Hänel et al, 2019; Lazova et al, 2012) because it does not require tissue disrupting direct ionization but rather the use of nonthermal pulsed electric fields, which do not lead to skin damage, scarring, or other potential medical risks (Golberg et al, 2016, 2018, 2013).

RESULTS

Workflow of proteomics sampling with e-biopsy from excised human skin and its analysis

e-biopsy for proteome sampling from freshly (10−20 minutes since the time of excision) excised human skin is shown in Figure 1a. First, the sampling needle is inserted (1−2 mm penetration depth) in the sampling location, the ground needle is positioned on the skin surface (without penetration), and the pulsed electric fields are applied. Second, a vacuum is applied on the same needle through which the pulsed electric field pulses are delivered, to pump the released cellular content into the needle and the syringe. Next, the tissue extract (∼1−3 μl) is discharged from the syringe to the external buffer (biology grade water) and subjected to standard protocols for molecular analysis, including purification, separation, identification (liquid chromatography with tandem mass spectrometry in this case), and quantification. Next, differential expression analysis was performed to determine a molecular signature that differentiates between BCC, cSCC, and keratosis lesions. Finally, obtained results were validated with the other protein extraction method, external transcriptomic dataset, and the immunohistochemical staining of the most differentially expressed protein.

e-biopsy sampling was applied in 3 positions in the same area of the tissue sample excised with conventional biopsy (tissue weight was 15−350 mg depending on the sample). The reproducibility of the e-biopsy methodology was evaluated (Supplementary Materials and Methods), calculating maximal intrapatient Pearson correlation between proteomes measured in each sampled patient's location. We observed Pearson correlation of 0.871 ± 0.082 (0.888 ± 0.067 for patients with BCC, 0.858 ± 0.079 for patients with SCC, and 0.863 ± 0.127 for patients with solar AK), which indicates high consistency of the e-biopsy sampling technique (Supplementary Table S1). Importantly, the inherent tissue spatial heterogeneity limits the ideal sampling method from receiving the exact measurement replicated in the proximate locations.

Modeling electric field in the human skin with tumors during e-biopsy

Numerical modeling is a computational tool that allows prediction of electric field and thermal distributions in physiologically complex structures. In this model (Figure 1b and c), we selected the electric field strength of 480 V cm^{-1} as a threshold for skin reversible electroporation (Čorović et al, 2012). The threshold selected for the irreversible skin electroporation was $E_{irev} = 1050 \frac{V}{cm}$ (Čorović et al, 2012). In addition, to estimate the potential thermal effects of the application of high-voltage pulsed electric fields on a skin tissue, we coupled the direct current model with the transient heat field problem (Figure 1b and d). The maximum predicted temperature increase was 2.2 $°C$, reaching 27.2 $°C$ relative to the initial temperature of 25 .0 $°C$ (black dot on Figure 1d).

e-biopsy sampled proteome, validated by conventional biopsy, differentiates cSCC from BCC in human skin

Datasets. To assess the data potential in distinguishing between cSCC, BCC, and benign lesions proteomic profiles, we used a dataset of 48 patients, specifically 21 patients with cSCC, 20 patients with BCC, and 7 patients with solar AK with similar sex, age, and birth origin distributions (Supplementary Table S2 and Supplementary Figure S1). Each patient's lesion was sampled with e-biopsy technique in 3 locations, resulting respectively in 63 and 60 samples per carcinoma type together with 21 noncarcinoma samples. In total, we identified 5966 proteins observed with nonzero intensity in at least 1 of 144 dataset samples (Figure 2). In our analyses, we addressed both raw liquid chromatography with tandem mass spectrometry measurements and the corresponding binary protein appearance patterns (constructed as binary vectors, with 1 associated with positively measured protein intensity in the sample).

For validation, protein identification through liquid chromatography with tandem mass spectrometry measurements was conducted on samples obtained from the same group of patients. Specifically, 38 samples were taken from 20 patients with BCC, and 33 samples were obtained from 21 patients with cSCC, with at least 1 sample collected from each patient, as shown in Supplementary Table S2. It is important to note that a conventional tissue lysis protocol was used to extract the proteins. It is essential to consider that significantly larger tissue areas were used for these lysis measurements, potentially resulting in a mixture of various cellular conditions and subtypes being amalgamated into a single bulk measurement of cells.

For additional validation, we used an external transcriptomic dataset published by Wan et al (2021), which reports transcript counts per million for 16,382 genes in 25 patients with BCC and 10 patients with cSCC. Similar to our lysis measurements, these samples were obtained from the relatively large tissue areas, which could span over a mixture of different cellular conditions. Specifically, Wan et al (2021) report working with tissues with tumor content above 30%, which was measured on the basis of examination of corresponding tissue images.

All the raw proteomics data are available online through ProteomeXchange with identifier PXD046711 and in Supplementary Table S3, whereas patient diagnoses are available in Supplementary Table S2.

Differential expression analysis. To identify the most differentially expressed proteins, we performed a parametric (Student *t*-test) (Supplementary Figure S2 and Supplementary Table S4) and nonparametric (Mann−Whitney *U* test) (Supplementary Figure S3 and Supplementary Table S4)

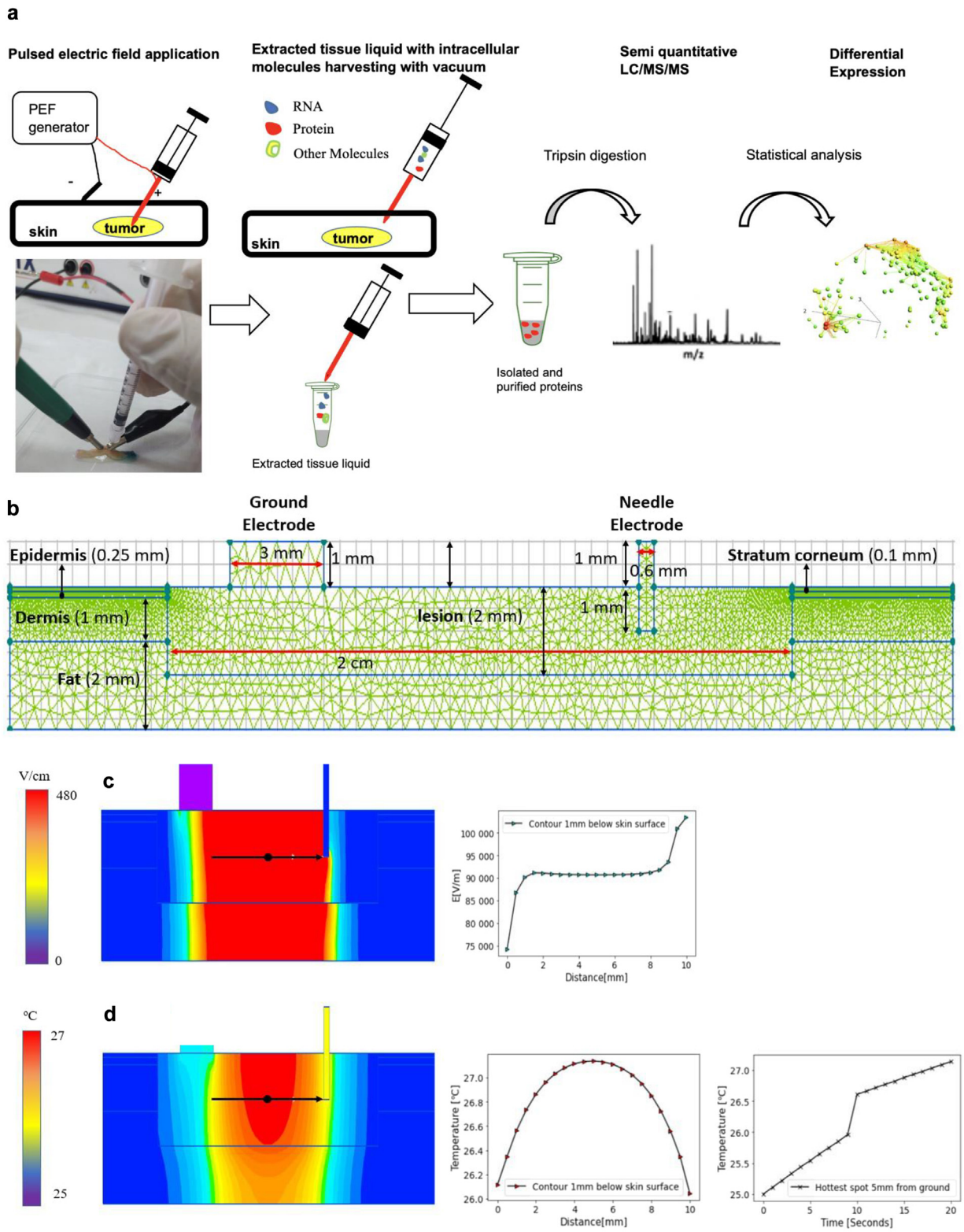

Figure 1. e-biopsy procedure for skin molecular sampling. (**a**) Skin e-biopsy procedure ex vivo. Schematics of molecular harvesting with e-biopsy is shown. **(b)** Model geometry. Skin layers are comprised of stratum corneum, epidermis, and dermis, followed by fat layer; each layer has its own electrical properties, presented in Supplementary Table S7. In this model, a tumor penetrates 2 mm, and clear skin layers route into fat layer, and alongside are lesion left and right boundaries and 5-mm healthy skin tissue. Actual geometric proportions are not preserved here for visualization purposes. **(c)** The electric field distribution in a lesion while applying 1000 V, with a color map of the electric field strength. Red color represents the electroporated tissue area ($E > 480$ V cm^{-1}), which is mainly located between ground and needle electrodes (right). An electric field strength profile between ground electrode to needle electrode is shown, 1 mm below lesion surface (left) **(d)** Left: analysis of temperature distribution after 2 sequential pulses: high and rapid followed by slow and longer pulses. Shown is a transient heat transfer problem created through coupling of DC conduction problem when V = 1000 SV was applied, V_{rms} = 12.65 V, pulsing for 10 seconds, with steady-state heat transfer problem with confined Dirichlet boundary conditions. The described transient heat problem was coupled after 10 seconds

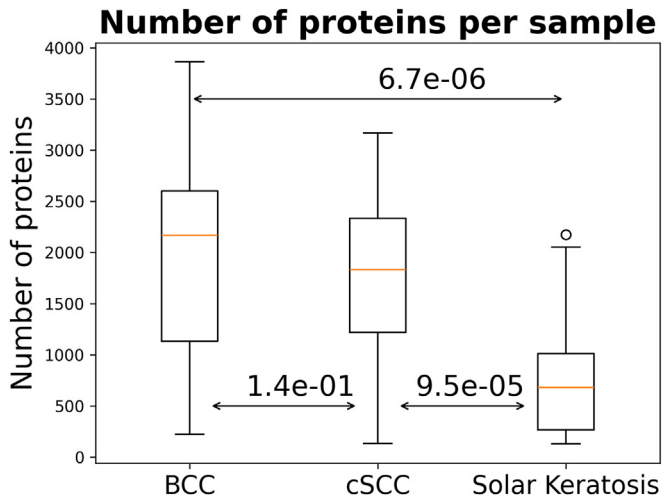

Figure 2. Number of proteins identified with e-biopsy per sample in BCC, cSCC, and solar AK measurements. The number above arrows correspond to *P*-value of Student *t*-test comparison between distributions. ANOVA *P*-value for these 3 groups is 1.5e-05. The box corresponds to IQR in data (from quartile 1 to quartile 3), the orange line shows the median, and the whiskers extend from the box to the farthest data point lying within 1.5× IQR. AK, actinic keratosis; BCC, basal cell carcinoma; cSCC, cutaneous squamous cell carcinoma; e-biopsy, electroporation-based biopsy; IQR, interquartile range.

statistical comparisons together with the comparison of binary appearance patterns (Supplementary Materials and Methods) (Vitkin proportion-based test [Vitkin, 2024]) (Supplementary Figure S4 and Supplementary Table S4) between cSCC and BCC samples on intensity-based absolute quantification (iBAQ) (Supplementary Materials and Methods) intensity measurements.

All tests identified a high number of significantly differentiated proteins in each comparison pair (Table 1 and Supplementary Table S5). We identified 3 genes (*CRNN*, *SULT1E1*, and *ITPK1*) that significantly changed (overexpressed with change of means >4 folds) (Table 2 and Figure 3) in BCC compared with those in cSCC even after a most conservative (Bonferroni) correction for multiple testing (Materials and Methods). Aggregating sample data on a patient level did not result in any genes with significant change (after Bonferroni correction). The most probable reason for this is the reduced sizes of compared populations: 21 versus 20 patients instead of 63 versus 60 samples. However, the overall protein expression changes between BCC and cSCC groups remained consistent both in observed proportions and in measured means.

In validation data, very similar significant changes in each of these genes were observed in proteomic validation samples collected by conventional tissue biopsy (Figure 3) as well as in transcriptomics data reported by Wan et al (2021) (Table 2 and Figure 3).

Comparison with solar AK data collected with e-biopsy showed that all 3 genes are significantly higher both in BCC and in SCC than in solar AK. *SULT1E1* and *ITPK1* were not observed in solar AK samples collected with e-biopsy, whereas *CRNN* was observed only in 5 (24%) of the samples, corresponding to 3 (43%) of patients with solar AK. Moreover, its average iBAQ measurement in BCC and cSCC was significantly higher than in solar AK, with 152-fold ($P = 1.3e-6$) and 13-fold ($P = .2$) for BCC and SCC, respectively (Figure 3 and Supplementary Table S5).

Comparing proteomes sampled through e-biopsy with those extracted through conventional biopsy lysis methods and published transcriptomic data

Comparative validation of proteomic measurements in samples collected with e-biopsy method with the samples collected with conventional biopsy lysis method (Supplementary Table S6) reveals high agreement in protein appearance patterns between obtained measurements. Both for BCC and for cSCC, we achieve Spearman R = 0.81 ($P < 1e-323$) for similarity between proportion vectors (vectors counting for each protein the percentage of samples in which it was identified). Figure 4a displays the proportions for 10 proteins identified as the most different between BCC and cSCC. It is noteworthy that 9 of these vectors are overexpressed in BCC, whereas SERPINB13 shows overexpression in cSCC. Interestingly, SERPINB13 is completely absent in BCC e-biopsy–collected samples but is marginally detected in samples extracted with conventional lysis biopsy (Figure 4a). These variations and similar discrepancies may be attributed to the significantly larger tissue volumes collected through the standard lysis technique, which inherently captures potential tissue heterogeneity.

Comparison of measured intensities also shows high agreement in expression patterns between e-biopsy and lysis techniques. Both for BCC and for cSCC, we achieve Spearman R = 0.83 ($P < 1e-323$) for similarity between average measurement vectors (vectors with mean iBAQ measurement for each protein). Moreover, we observe meaningful agreement with transcriptomics measurements (Wan et al, 2021) (Spearman R = 0.29 [$P = 2.3e-103$] and Spearman R = 0.34 [$P = 1.5e-141$] for BCC and cSCC, respectively). Figure 4b displays mean iBAQ proteomic and counts per million transcriptomic measurements for 10 proteins identified as most different between BCC and cSCC. Note that BCC−cSCC relative directions of 9 of these proteins (except for keratin 27) agree between e-biopsy and lysis samples. Moreover, these directions agree with the directions observed in transcriptomics data in all 10 proteins.

The first disagreements in BCC−cSCC relative directions between e-biopsy proteomics and published transcriptomics data appear in the second decile of proteins identified as most different between BCC and cSCC. Among 20 such proteins (Supplementary Table S5), we discover 4 such genes: O00425 (gene *IGF2BP3*), P35749 (gene *MYH11*), P49643 (gene *PRIM2*, DNA primase large subunit), and Q01415 (gene *GALK2*, N-acetylgalactosamine kinase).

pulsing, with another DC conduction problem when V = 50V was applied, V_{rms} = 10 V, pulsing for 10 seconds to create a transient heat transfer problem performed in a and d. Middle: the temperature profile from the ground electrode until the needle electrode. Right: temperature increase in time at the point located 1 mm beneath the electrode. DC, direct current; e-biopsy, electroporation-based biopsy; LC/MS/MS, liquid chromatography with tandem mass spectrometry; PEF, pulsed electric field.

Table 1. Number of Proteins Identified in e-biopsy Setup as Significantly ($P < 5\%$) Differentially Expressed by Any of the 3 Tests

Group A	Group B	Up in A <5%	Up in B <5%	Overall <5%	FDR <5%	Bonferroni Corrected <5%
BCC	cSCC	870	224	1094	0.27	3
BCC	Solar AK	2693	100	2793	0.11	38
cSCC	Solar AK	1976	53	2029	0.15	3

Abbreviations: AK, actinic keratosis; BCC, basal cell carcinoma; cSCC, cutaneous squamous cell carcinoma; e-biopsy, electroporation-based biopsy; FDR, false discovery rate.

Validation of cornulin expression differences between BCC and cSCC by immunohistochemistry staining

We performed an immunohistochemistry staining for the most differentially expressed (per sample) protein between BCC and cSCC: cornulin (gene *CRNN*, Uniport identification Q9UBG3). The staining was done in 4 patients with BCC and 4 patients with cSCC selected among the same 41 patients. Immunohistochemistry staining results confirmed significantly higher CRNN identified in BCC tumor (scored 4, corresponding to moderate immune reaction [25−50 positive cells]) than CRNN identified in cSCC tumor (scored 1.25, where score 1 corresponds to only a few positive cells [<5 cells]), as presented in Figure 5.

DISCUSSION

The clinical diagnoses of cSCC and BCC are performed by a direct skin inspection (Mohammad et al, 2015), often assisted by dermoscopy (Sinz et al, 2017). In addition, multiple emerging methods such as optical coherence tomography (Ferrante di Ruffano et al, 2018), reflectance confocal microscopy (Pellacani et al, 2019), elastic scattering spectroscopy (Rodriguez-Diaz et al, 2019), and high-frequency ultrasound (Chen et al, 2022) aim to assist the clinician in diagnosis. Nevertheless, conventional tissue biopsy for histopathological analysis is still essential to confirm the diagnosis, to estimate the risk of recurrence, and to further dictate the treatment pathway (Tanese, 2019). Skin structural and functional complexity led to existence of multiple types of biopsies, with major methods including punch biopsy, shave biopsy, excisional biopsy, and curettage biopsies (Crowson et al, 2010).

The clinical features of cSCC and BCC are well-described, and in most cases, the clinical diagnosis is done according to the subsequent histologic verification. Sometimes, however, the clinical phenotypes of these cancers are ambiguous, and discrepancies between the clinical presentations and histologic analyses occur (Neagu et al, 2020; Ryu et al, 2018). Such misclassification of cSCC as BCC (or vice versa) affects the treatment plan of the lesion (Mohammad et al, 2015). Misclassification of cSCC as BCC carries the highest risk to patients owing to the inherent potential for recurrence, metastases, and mortality (Lallas et al, 2015). Recent studies suggested that the introduction of molecular biomarkers, which would accurately stratify nonmelanoma skin lesions, would provide a new frontier in personalization of skin cancer care and hold a potential of greatly improving patient diagnosis in many cases (Azimi et al, 2020). Besides the algorithms for discovery of the specific molecular signatures for each of the diseases, the yet open challenge is the sampling of biomarkers. The current strategy involves molecules extraction using lyses buffers from tissue sample with tissue biopsies. Conventional tissue biopsy procedures carry risks involved with surgical procedures and may lead to localized tissue injury, bleeding, inflammation, infection, and scarring (Abhishek and Khunger, 2015). In addition, because of these risks, only a few biopsies can be performed in a single procedure, limiting the scope of the spatial mapping of the entire lesion, potentially leading to misdiagnosis if the tumor is only partially sampled or completely missed (Wolberink et al, 2013). To address these problems and to allow direct molecular sampling from tissue without resection, a series of procedures and associated mass spectrometric tools are currently under development (Hänel et al, 2019), yet none of these to date have received a broad community recognition. These include intelligent knife, desorption electrospray ionization (Margulis et al, 2018), picosecond infrared laser, and the MasSpec pen (Chan, 2019; Hänel et al, 2019). All these methods require high energy for sample evaporation, potentially damaging the tissue (Hänel et al, 2019). In addition, the ionization process is competitive, thus not all informative molecules will be sampled (Hänel et al, 2019).

The e-biopsy aims to extend the state-of-the-art technologies that will potentially enable precision diagnosis and therapy using low-energy and low-temperature molecular sampling (Figure 1). Interestingly, our study showed that e-biopsy−sampled proteomes are different between BCC and cSCC, with 1094 of identified proteins displaying significant expression changes (870 higher in expressed BCC and 224 higher expressed in cSCC; false discovery rate = 0.27). Moreover, changes in CRNN, SULT1E1, and ITPK1 protein expression patterns were significant even after the Bonferroni correction for multiple testing. Furthermore, the analysis of transcriptomic data of Wan et al (2021) confirms significant overexpression of these 3 proteins in BCC compared with those in cSCC (Table 2).

Some of these proteins were shown to be related to cancer. For example, Cornulin, (*CRNN* gene; Mann−Whitney *U* test $P = 6.1E\text{-}08$, fold change =11.9), downregulated in cSCC in comparison with that in BCC, plays a role in epidermal differentiation, whereas its expression is believed to be specific to squamous cells (Contzler et al, 2005). It was shown previously that CRNN is downregulated in tongue cSCC (Xu et al, 2000; Ye et al, 2008). Upregulated CRNN levels prevent lesion formation, and its tumor suppressive role has been reported (Chen et al, 2013), which is aligned with the less aggressive nature of BCC. SULT1E1 (Mann−Whitney *U* test

Table 2. BCC Versus cSCC Comparison of e-biopsy Proteomics Measurements

Number	Gene Name	per	e-biopsy measurements: BCC Proportion, %	BCC Mean	cSCC Proportion, %	cSCC Mean	Minimal *P*-Value	Bonferroni-Corrected Minimal *P*-Value	Log_2 Fold Change	Average Transcript CPM Based on Wan et al (2021): Mean BCC Count	Mean cSCC Count	Log_2 Fold Change	*t*-Test *P*-Value
1	*CRNN*	Sample	82%	2.07E + 07	35%	1.74E + 06	6.13E-08	1.10E-03	3.57	386.63	17.16	4.49	1.23E-02
		Patient	100%	6.22e + 07	62%	5.23e + 06	2.12e-04	1					
2	*SULT1E1*	Sample	55%	2.76E + 06	13%	1.29E + 05	4.90E-07	8.76E-03	4.41	74.24	3.53	4.39	6.68E-05
		Patient	80%	8.28e + 06	29%	3.88e + 05	4.13e-04	1					
3	*ITPK1*	Sample	43%	4.84E + 05	6%	1.13E + 05	1.80E-06	3.23E-02	2.10	189.55	41.79	2.18	4.68E-06
		Patient	70%	1.45e + 06	10%	3.38e + 05	7.25e-05	1					

Abbreviations: BCC, basal cell carcinoma; CPM, count per million; cSCC, cutaneous squamous cell carcinoma; e-biopsy, electroporation-based biopsy.
Most significantly (according to *P*-value) changed proteins are shown.

$P = 4.9E-07$, fold change = 21.3), which also appears in BCC with increased measured intensity in comparison with cSCC, is responsible for the metabolism of active estrogens and plays crucial roles in their homeostasis (Yi et al, 2021). SULT1E1 downregulation was proposed to serve as a marker for more aggressive cancer (Xu et al, 2018). ITPK1 (Mann–Whitney *U* test $P = 5.7E-06$, fold change = 4.3) regulates the synthesis of inositol phosphates, which are substrates for inositol polyphosphate-5-phosphatase, an enzyme that was shown to play a role in the progression of AK to cSCC (Maly et al, 2020). These findings imply further investigation of inositol metabolism in cSCC. Additional studies for the dissection of the biological role of all identified proteins are needed.

The decision to perform a conventional skin lesion biopsy should only be made if it provides essential diagnostic information to the clinician. A proposed e-biopsy technique could introduce a sampling approach for personalized medicine, offering a minimally invasive precondition to determine the necessity of conventional tissue biopsy on the basis of local molecular information e-biopsy has the potential to personalize the care of skin and other solid tumors, potentially reducing morbidity and mortality by expediting decisions on advanced surgeries or additional therapies such as radiation, chemotherapy, or emerging immunotherapy. It can also help to determine follow-up visit frequency and the type of imaging required. Currently, there are no approved biomarkers to distinguish high-risk nonmelanoma skin cancer from the benign subtypes. e-biopsy, with its ability to sample molecular signatures in vivo, may enable the classification of molecular signatures of skin and other solid tissue cancers on the basis of multiomics data and tumor characteristics, such as aggressiveness. For example, one potential aspect of e-biopsy is to potentially identify a biomarker for tumors that do have a metastatic potential.

These suggestions require future larger-scale studies for demonstration. Although this study showed the ability of e-biopsy to sample proteomes signatures, which differentiate between BCC and cSCC, to enable clinical decision, much more information and studies are needed. For example, the information of tumors subtypes, some of which are treated similar today for BCC and cSCC, is missing and requires follow-up studies. For example, in situ squamous cell carcinoma and superficial BCC are treated the same way and have similar implications for clinical outcomes. On the other hand, an invasive squamous cell carcinoma and infiltrative BCC would both require surgical management. In addition, additional risk factors for squamous cell carcinomas associated with poor outcomes should be included for follow-up classifiers (Thompson et al, 2016; Zakhem et al, 2023). Combining molecular measurements with patient demographics, tumor subtypes, and clinical information on patient's background and outcomes can pave the way for personalized diagnostics, more precise treatments, improved outcomes, and cost savings.

MATERIALS AND METHODS

From March 2020 to March 2022, tissue samples were collected from nonmelanoma skin cancer lesions from 48 patients who

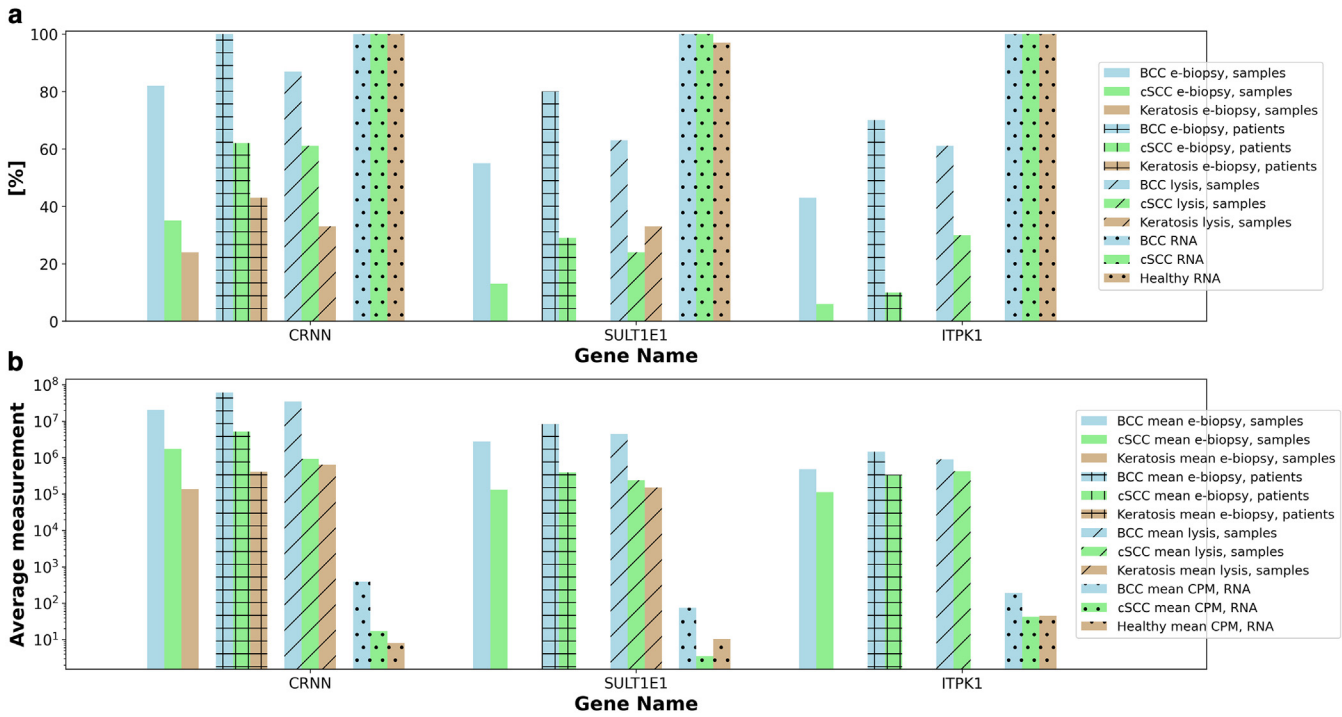

Figure 3. Statistics on protein measurement. (**a**) Proportion of samples per patients with positive measurement. Proportion of 80% refers to the fact that the gene was observed with positive intensity in 80% of samples. (**b**) Mean iBAQ measurement (in case of proteomics) and mean CPM (in case of transcriptomics by Wan et al [2021]). Lysis refers to measurements obtained by the lysis of samples obtained with conventional biopsy. BCC, basal cell carcinoma; CPM, count per million; cSCC, cutaneous squamous cell carcinoma; e-biopsy, electroporation-based biopsy; iBAQ, intensity-based absolute quantification.

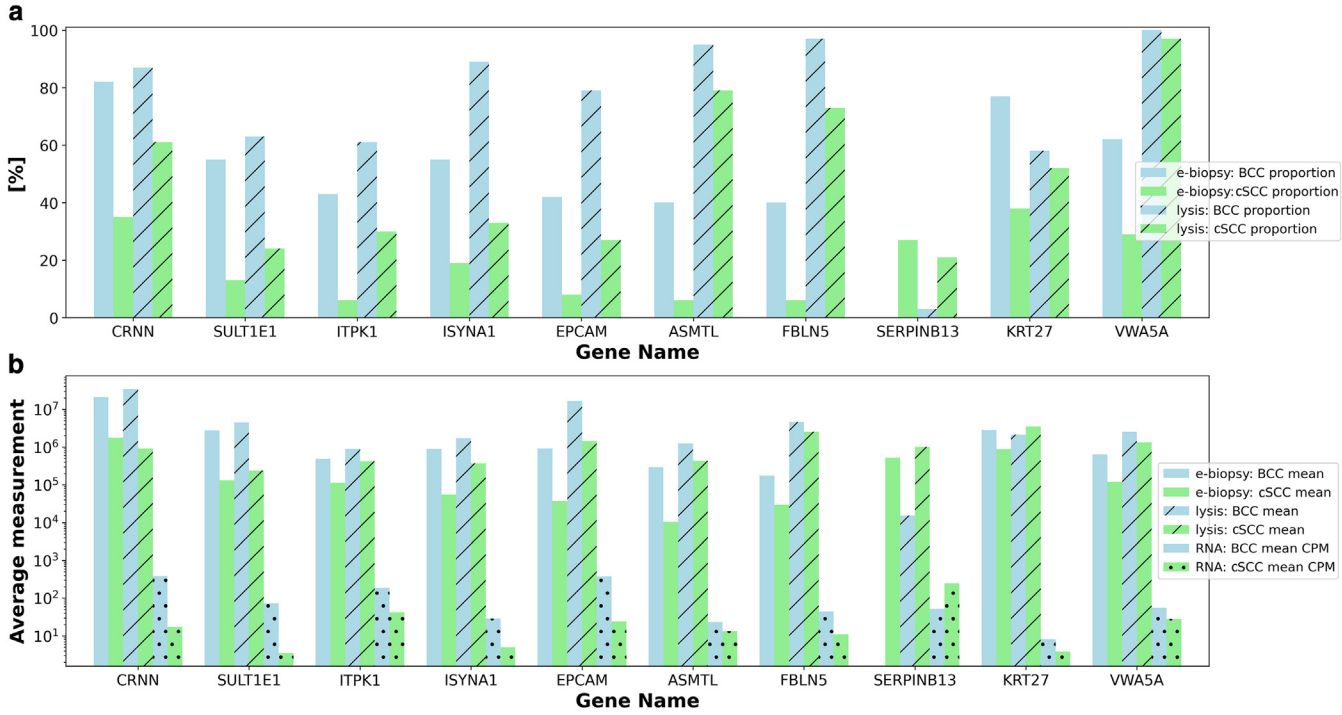

Figure 4. Comparative lysed conventional biopsy-extracted sample measurements of top 10 most differentiated proteins in BCC versus cSCC according to e-biopsy–collected samples. (**a**) Proportion of samples with positive measurement (transcriptomics is omitted because RNA was identified in all samples) (Supplementary Table S5). (**b**) Mean iBAQ measurement (in case of proteomics) and mean CPM (in case of transcriptomics by Wan et al [2021]). BCC, basal cell carcinoma; CPM, count per million; cSCC, cutaneous squamous cell carcinoma; e-biopsy, electroporation-based biopsy; iBAQ, intensity-based absolute quantification.

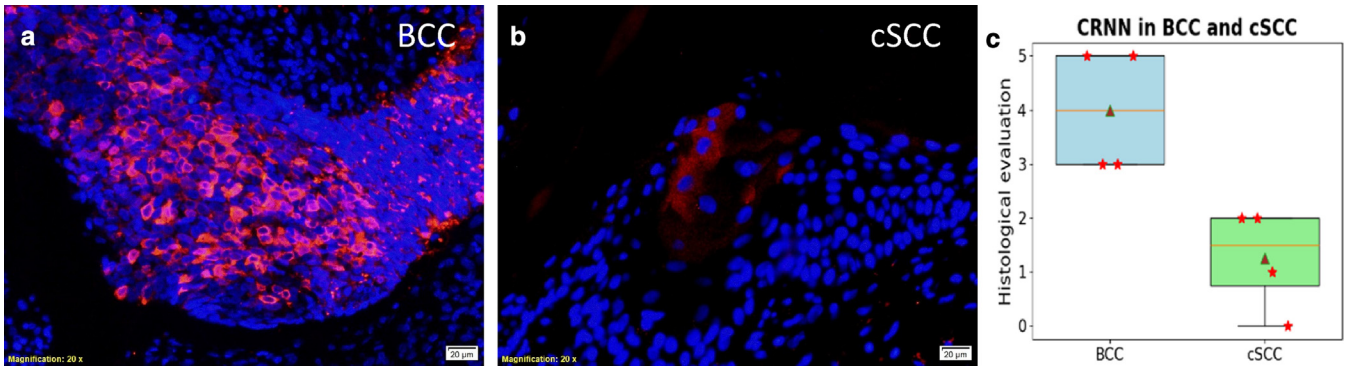

Figure 5. Immunostaining for CRNN. (**a**) Typical BCC slide. (**b**) Typical cSCC slide. (**c**) Semiquantitative immunohistochemistry staining results (Student *t*-test $P = .01$). Red stars correspond to single staining samples; triangle indicates mean staining score. The box corresponds to IQR in data (from quartile 1 to quartile 3), the orange line shows the median, and the whiskers extend from the box to the farthest data point lying within 1.5× IQR. BCC, basal cell carcinoma; cSCC, cutaneous squamous cell carcinoma; IQR, interquartile range. Scale bar = 20um.

underwent surgical excision of a skin lesion at Meir Medical Center (Kfar Sava, Israel). All lesions excised were at least 1 cm in diameter. Proteins were extracted fresh from 21 patients with cSCC, 20 patients with BCC, and 7 patients with solar AK (pathologically confirmed diagnoses) 10–20 minutes after surgery. This study was approved by the Meir Medical Center Institutional Review Board (number MMC-19-0230). All patients gave written consent for participation and genetic analysis of tissues.

Proteome extraction with e-biopsy

Each patient's lesion was sampled in 3 locations, resulting in 63 samples for cSCC, 60 samples for BCC, and 21 solar AK. The sampling needle (30-G insulin syringe) is inserted in the sampling location, and the ground needle is positioned 5 mm apart on the skin surface without penetration, and the pulsed electric fields are applied using our laboratory high-voltage pulsed electric field generator (Levkov et al, 2019) (Figure 1a). e-biopsy was performed using 2 steps (Ghosh et al, 2019; Golberg et al, 2019) as follows: 40 pulses, 1000 V, 40 μs, and 4 Hz and 40 pulses, 50 V, and 5 ms delivered at 4 Hz. The extracted liquids were immediately transferred to 1.5 ml tubes with 100 μl double-distilled water. Proteins were isolated from the e-biopsy extract using the EZ- RNA II kit (Biological Industries) and identified with liquid chromatography with tandem mass spectrometry performed using Q-Exactive Plus mass spectrometer (Thermo Fischer Scientific) and then analyzed using the MaxQuant software, version 1.5.2.8, with human proteome from the UniProt database with 1% false discovery rate (Supplementary Materials and Methods). To model the distribution of the electric fields in the skin with tumors during e-biopsy, we used the finite elements method in QuickField (Terra Analysis) (Supplementary Materials and Methods).

Proteome extraction with lysis of conventional biopsy samples

One sample from each lesion processed with a commercial EZ-RNA II kit was used for protein isolation. Each sample was homogenized in the denaturing solution (0.5 ml/50–100 mg tissue) using Bead Beater (BioSpec Products, Bartlesville, OK) followed by phase separation using 0.09 ml of 1-bromo-3-chloropropane and 0.4 ml water-saturated phenol, provided in the kit. The proteins were precipitated using isopropanol and washed later with 0.3 M guanidine hydrogen chloride in 95% ethanol. The protein pellets were air dried and taken for proteomic analysis.

Bioinformatics data analysis

Protein pairwise (BCC vs cSCC, BCC vs solar AK, and cSCC vs solar AK) differential expression analysis of samples was performed on iBAQ (Supplementary Materials and Methods) intensity measurements with a parametric Student *t*-test (scipy.stats.ttest_ind), with a nonparametric Mann–Whitney *U* test (scipy.stats.mannwhitneyu), and with a comparison of binary appearance pattern (Vitkin proportion-based test [Vitkin, 2024]) tests (Supplementary Materials and Methods). Protein expression fold change was defined as a ratio of iBAQ means clipped to the range of (1e-6; 1e6). To construct volcano plot visualizations (Supplementary Figures S2b, S3b, and S4b), both fold changes and test *P*-values were log transformed. To identify the strongest possible signal for each protein, we selected the minimum between 3 *P*-values and corrected it for multiple testing with the Bonferroni approach following Bland and Altman (Bland and Altman, 1995) by multiplying the *P*-value by 3 × 5966 (number of differential expression tests × number of identified proteins). False discovery rate (Table 1) was calculated for the 5% *P*-value cut, resulting in 298.3 randomly expected significant proteins.

Results validation with lysis of conventional biopsy samples and with external RNA dataset

Results validation was performed by comparison with (i) proteomics obtained by conventional tissue lysis procedure on the same patients (38 samples over 20 patients with BCC and 33 samples over 21 patients with cSCC, at least 1 sample per patient) (Supplementary Table S2) and (ii) external transcriptomic dataset published by Wan et al (2021), which reports transcript counts per million for 16,382 genes in 25 patients with BCC and 10 patients with cSCC.

ETHICS STATEMENT

This study was approved by the Meir Medical Center Institutional Review Board (number MMC-19-0230). All patients gave written informed consent for participation and genetic analysis of tissues.

DATA AVAILABILITY STATEMENT

The authors hereby declare that all data supporting the findings of this study are available within the paper and its supplementary materials. The mass spectrometry proteomics data have been deposited to the ProteomeXchange Consortium through the PRIDE partner repository, with the dataset identifier PXD050713. The proteomes data are available in PRIDE depository (identification PXD046711; http://www.ebi.ac.uk/pride/archive/projects/PXD050713). The complete code for the used numerical models is available at https://github.com/GolbergLab/BCCvsSCC.git.

ORCIDs

Edward Vitkin: http://orcid.org/0000-0003-4055-4772

Julia Wise: http://orcid.org/0009-0008-0575-270X
Ariel Berl: http://orcid.org/0000-0003-3705-5454
Ofir Shir-az: http://orcid.org/0000-0001-7942-6394
Batel Gabay: http://orcid.org/0009-0004-3922-2708
Amrita Singh: http://orcid.org/0000-0002-8551-7708
Vladimir Kravtsov: http://orcid.org/0000-0002-4017-1387
Zohar Yakhini: http://orcid.org/0000-0002-0420-5412
Avshalom Shalom: http://orcid.org/0000-0003-2074-1650
Alexander Golberg: http://orcid.org/0000-0001-8782-8879

CONFLICT OF INTEREST

A patent application was filed to protect the electroporation-based sampling technology described in this study as invented by AG, JS, and ZY. EV, AG, JS, AS, and ZY have interest in Elsy Medical. The remaining authors state no conflict of interest.

ACKNOWLEDGMENTS

The authors thank the Israel Ministry of Science and Technology, Israel Innovation authority Kamin project, the TAU SPARK fund, TAU Zimin Center for technologies for better life, and the EuroNanoMed MATISSE project for their support of this project. All authors thank the members of the Smoler Proteomics Center at the Faculty of Biology at the Technion - Israel Institute of Technology. The authors specifically thank Keren Bendalak for her help with the liquid chromatography with tandem mass spectrometry analysis.

AUTHOR CONTRIBUTIONS

Conceptualization: EV, ZY, AS, AG; Investigation: JW, AB, OS, VK, AS, AS, AG; Methodology: AG, EV, AS; Writing - Original Draft Preparation: EV, BG, AG; Writing - Review and Editing: AB, ZY, AS, EV, AG

DECLARATION OF GENERATIVE ARTIFICIAL INTELLIGENCE (AI) OR LARGE LANGUAGE MODELS (LLMs)

The author(s) did not use AI/LLM in any part of the research process and/or manuscript preparation.

SUPPLEMENTARY MATERIALS

Supplementary material is linked to the online version of the paper at www.jidonline.org, and at https://doi.org/10.1016/j.xjidi.2024.100304.

REFERENCES

Abhishek K, Khunger N. Complications of skin biopsy. J Cutan Aesthet Surg 2015;8:239–41.

Azimi A, Yang P, Ali M, Howard V, Mann GJ, Kaufman KL, et al. Data independent acquisition proteomic analysis can discriminate between actinic keratosis, Bowen's disease, and cutaneous squamous cell carcinoma. J Invest Dermatol 2020;140:212–22.e11.

Balog J, Sasi-Szabó L, Kinross J, Lewis MR, Muirhead LJ, Veselkov K, et al. Intraoperative tissue identification using rapid evaporative ionization mass spectrometry. Sci Transl Med 2013;5:194ra93.

Bland JM, Altman DG. Multiple significance tests: the Bonferroni method. BMJ 1995;310:887–91.

Chan LSY. Mohs Micrographic Surgery Sine Microscopy: is mass spectrometry an upcoming intraoperative cancer margin assessment tool? Sci Repos 2019;1:1–3.

Chen K, Li Y, Dai Y, Li J, Qin Y, Zhu Y, et al. Characterization of tumor suppressive function of cornulin in esophageal squamous cell carcinoma. PLoS One 2013;8:e68838.

Chen ZT, Yan JN, Zhu AQ, Wang LF, Wang Q, Li L, et al. High-frequency ultrasound for differentiation between high-risk basal cell carcinoma and cutaneous squamous cell carcinoma. Skin Res Technol 2022;28:410–8.

Contzler R, Favre B, Huber M, Hohl D. Cornulin, a new member of the "fused gene" family, is expressed during epidermal differentiation. J Invest Dermatol 2005;124:990–7.

Čorović S, Mir LM, Miklavčič D. In vivo muscle electroporation threshold determination: realistic numerical models and in vivo experiments. J Membr Biol 2012;245:509–20.

Crowson A. Neil, Magro CM, Mihm MC. Biopsy interpretation of the skin : primary non-lymphoid cutaneous neoplasia. Philadelphia: Lippincott Williams & Wilkins; 2010. p. 455.

Ferrante di Ruffano L, Dinnes J, Deeks JJ, Chuchu N, Bayliss SE, Davenport C, et al. Optical coherence tomography for diagnosing skin cancer in adults. Cochrane Database Syst Rev 2018;2018:CD013189.

Genish I, Gabay B, Ruban A, Goldshmit Y, Singh A, Wise J, et al. Electroporation-based proteome sampling ex vivo enables the detection of brain melanoma protein signatures in a location proximate to visible tumor margins. PLoS One 2022;17:e0265866.

Ghosh S, Gillis A, Sheviryov J, Levkov K, Golberg A. Towards waste meat biorefinery: extraction of proteins from waste chicken meat with non-thermal pulsed electric fields and mechanical pressing. J Clean Prod 2019;208:220–31.

Golberg A, Broelsch GF, Bohr S, Mihm MC Jr, Austen WG Jr, Albadawi H, et al. Non-thermal, pulsed electric field cell ablation: A novel tool for regenerative medicine and scarless skin regeneration. Technology (Singap World Sci) 2013;1:1–8.

Golberg A, Sheviryov J, Solomon O, Anavy L, Yakhini Z. Molecular harvesting with electroporation for tissue profiling. Sci Rep 2019;9:15750.

Golberg A, Villiger M, Felix Broelsch G, Quinn KP, Albadawi H, Khan S, et al. Skin regeneration with all accessory organs following ablation with irreversible electroporation. J Tissue Eng Regen Med 2018;12:98–113.

Golberg A, Villiger M, Khan S, Quinn KP, Lo WCY, Bouma BE, et al. Preventing scars after injury with partial irreversible electroporation. J Invest Dermatol 2016;136. 2297–04.

Hänel L, Kwiatkowski M, Heikaus L, Schlüter H. Mass spectrometry-based intraoperative tumor diagnostics. Future Sci OA 2019;5:FSO373.

Lallas A, Pyne J, Kyrgidis A, Andreani S, Argenziano G, Cavaller A, et al. The clinical and dermoscopic features of invasive cutaneous squamous cell carcinoma depend on the histopathological grade of differentiation. Br J Dermatol 2015;172:1308–15.

Lazova R, Seeley EH, Keenan M, Gueorguieva R, Caprioli RM. Imaging mass spectrometry–a new and promising method to differentiate Spitz nevi from Spitzoid malignant melanomas. Am J Dermatopathol 2012;34:82–90.

Levkov K, Vitkin E, González CA, Golberg A. A laboratory IGBT-based high-voltage pulsed electric field generator for effective water diffusivity enhancement in chicken meat. Food bioproc tech. Food Bioprocess Technol 2019;12:1993–2003.

Maly CJ, Cumsky HJL, Costello CM, Schmidt JE, Butterfield RJ, Zhang N, et al. Prognostic value of inositol polyphosphate-5-phosphatase expression in recurrent and metastatic cutaneous squamous cell carcinoma. J Am Acad Dermatol 2020;82:846–53.

Margulis K, Chiou AS, Aasi SZ, Tibshirani RJ, Tang JY, Zare RN. Distinguishing malignant from benign microscopic skin lesions using desorption electrospray ionization mass spectrometry imaging. Proc Natl Acad Sci U S A 2018;115:6347–52.

Mohammad EA, Mansour M, Parichehr K, Farideh D, Amirhossein R, Ahmad SA. Assessment of clinical diagnostic accuracy compared with pathological diagnosis of basal cell carcinoma. Indian Dermatol Online J 2015;6:258–62.

Neagu N, Lallas K, Maskalane J, Salijuma E, Papageorgiou C, Gkentsidi T, et al. Minimizing the dermatoscopic morphologic overlap between basal and squamous cell carcinoma: a retrospective analysis of initially misclassified tumours. J Eur Acad Dermatol Venereol 2020;34:1999–2003.

Pellacani G, Scope A, Gonzalez S, Guitera P, Farnetani F, Malvehy J, et al. Reflectance confocal microscopy made easy: the 4 must-know key features for the diagnosis of melanoma and nonmelanoma skin cancers. J Am Acad Dermatol 2019;81:520–6.

Rodriguez-Diaz E, Manolakos D, Christman H, Bonning MA, Geisse JK, A'Amar OM, et al. Optical spectroscopy as a method for skin cancer risk assessment. Photochem Photobiol 2019;95:1441–5.

Ryu TH, Kye H, Choi JE, Ahn HH, Kye YC, Seo SH. Features causing confusion between basal cell carcinoma and squamous cell carcinoma in clinical diagnosis. Ann Dermatol 2018;30:64–70.

Sinz C, Tschandl P, Rosendahl C, Akay BN, Argenziano G, Blum A, et al. Accuracy of dermatoscopy for the diagnosis of nonpigmented cancers of the skin. J Am Acad Dermatol 2017;77:1100–9.

Tanese K. Diagnosis and management of basal cell carcinoma. Curr Treat Options Oncol 2019;2(20):1–13. Berlin: Springer.

Thompson AK, Kelley BF, Prokop LJ, Murad MH, Baum CL. Risk factors for cutaneous squamous cell carcinoma recurrence, metastasis, and disease-specific death: a systematic review and meta-analysis. JAMA Dermatol 2016;152:419–28.

Vitkin E, Singh A, Wise J, Ben-Elazar S, Yakhini Z, Golberg A. Nondestructive protein sampling with electroporation facilitates profiling of spatial differential protein expression in breast tumors in vivo. Sci Rep 2022;12:15835.

Vitkin E. Differential expression analysis of binary appearance patterns. Open Res Europe 2024;4:52.

Wan J, Dai H, Zhang X, Liu S, Lin Y, Somani AK, et al. Distinct transcriptomic landscapes of cutaneous basal cell carcinomas and squamous cell carcinomas. Genes Dis 2021;8:181–92.

Wolberink EA, Pasch MC, Zeiler M, van Erp PE, Gerritsen MJ. High discordance between punch biopsy and excision in establishing basal cell carcinoma subtype: analysis of 500 cases. J Eur Acad Dermatol Venereol 2013;27:985–9.

Xu Y, Lin X, Xu J, Jing H, Qin Y, Li Y. SULT1E1 inhibits cell proliferation and invasion by activating PPARγ in breast cancer. J Cancer 2018;9:1078–87.

Xu Z, Wang MR, Xu X, Cai Y, Han YL, Wu KM, et al. Novel human esophagus-specific gene c1orf10: cDNA cloning, gene structure, and frequent loss of expression in esophageal cancer. Genomics 2000;69:322–30.

Ye H, Yu T, Temam S, Ziober BL, Wang J, Schwartz JL, et al. Transcriptomic dissection of tongue squamous cell carcinoma. BMC Genomics 2008;9:69.

Yi M, Negishi M, Lee SJ. Estrogen sulfotransferase (SULT1E1): its molecular regulation, polymorphisms, and clinical perspectives. J Pers Med 2021;11:194.

Zakhem GA, Pulavarty AN, Carucci J, Stevenson ML. Association of patient risk factors, tumor characteristics, and treatment modality with poor outcomes in primary cutaneous squamous cell carcinoma: a systematic review and meta-analysis. JAMA Dermatol 2023;159:160–71.